



Blueshift of the silver plasmon band using controlled nanoparticle dissolution in aqueous solution

Mogensen, Klaus Bo; Kneipp, Katrin

Published in:
Proceedings of Nanotech 2014

Publication date:
2014

[Link back to DTU Orbit](#)

Citation (APA):
Mogensen, K. B., & Kneipp, K. (2014). Blueshift of the silver plasmon band using controlled nanoparticle dissolution in aqueous solution. In *Proceedings of Nanotech 2014*

General rights

Copyright and moral rights for the publications made accessible in the public portal are retained by the authors and/or other copyright owners and it is a condition of accessing publications that users recognise and abide by the legal requirements associated with these rights.

- Users may download and print one copy of any publication from the public portal for the purpose of private study or research.
- You may not further distribute the material or use it for any profit-making activity or commercial gain
- You may freely distribute the URL identifying the publication in the public portal

If you believe that this document breaches copyright please contact us providing details, and we will remove access to the work immediately and investigate your claim.

Blueshift of the silver plasmon band using controlled nanoparticle dissolution in aqueous solution.

Klaus B. Mogensen* and Katrin Kneipp**

* Technical University of Denmark (DTU), Dept. of Micro- and Nanotechnology, 2800 Kgs. Lyngby, Denmark, klaus.mogensen@nanotech.dtu.dk

** Technical University of Denmark (DTU), Dept. of Physics, 2800 Kgs. Lyngby, Denmark.

ABSTRACT

In this work, we report the size-dependent blue shift of the silver nanoparticle plasmon band in aqueous solution by means of UV/VIS spectroscopy. An oxidative dissolution scheme allows a gradual decrease in the particle sizes by controlled oxidation during recording of the optical spectra. Hence, all sizes until complete dissolution can be obtained on the same substrate, thereby avoiding substrate-to-substrate variations and greatly increasing the size resolution. Cyanide and cysteamine are strong nucleophiles (electron pair donors) that deposits negative charge onto the NP surface. A $1/R$ -dependence of the plasmon peak energy is seen, which is interpreted as an increase in the free electron density of the nanoparticles.

Utilization of the size-dependent electronic contribution to the optical response in nanoplasmonic sensors is shown to be a promising extension to improve the sensitivity and specificity, as compared to traditional refractive index sensing.

Keywords: plasmonics, biosensor, blue shift, nanoparticles, cyanide

1 INTRODUCTION

The optical properties of small metallic nanoparticles (NPs < 5 nm) have been studied for decades [1, 2]. There has, however, been an increasing interest in this subject in recent years [3-5], especially in relation to the electronic properties, where both blue and red shifts have been observed for a reduction in size.

Here, silver particles forming a nanoplasmonic film on glass substrates are used to demonstrate a $1/R$ -dependence of the peak energy as well as a saturation in the energy for small particles, using both electron density donors and acceptors in aqueous solution. These measurements are complementary to recent electron energy loss spectroscopy (EELS) studies of the plasmon band blueshift [3]. While the spatial resolution of EELS is very high, the energy resolution is poor and the technique is limited to particles in the gas phase. For future applications, e.g. as potential biosensors, the behavior in aqueous solution is of great interest. Measurements in the aqueous phase furthermore allows increased flexibility in relation to the study of surface screening effects on the peak position, due to the

large availability of ligands. The size dependence is typically investigated by synthesizing particles with different sizes and comparing their optical response. In this work, an alternative strategy is used. Controlled dissolution of the AgNPs are employed, while continuously measuring the plasmon band using UV/VIS spectroscopy, thereby significantly simplifying the experiment, while at the same time overcoming substrate-to-substrate variations. A much higher resolution in terms of size can be obtained, which makes it possible to more clearly distinguish between different optical regimes (extrinsic vs intrinsic [2] or surface vs bulk effects [4]), depending on the type of analyte.

Two different types of dissolution schemes are employed, based on the electron pair donating and oxidizing properties of the analytes, respectively. However, in both schemes, AgNPs are oxidized, resulting in release of Ag^+ ions into solution (Fig. 1) and a decrease in the AgNP size.

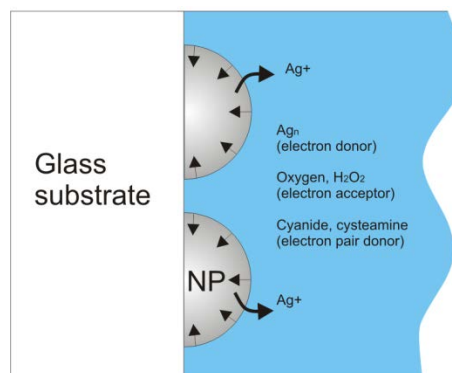


Figure 1. Sketch of the nanoparticle size reduction due to silver dissolution during measurements of the plasmon band. The nucleophile (cyanide or cysteamine) donates electron density to the NP surface that furthermore results in a blue shift of the plasmon band.

A blueshift in the plasmon band position upon oxidative dissolution has been observed previously for colloidal silver solutions by e.g. Henglein et. al [1], however not for nanoparticles on a substrate. Furthermore, a detailed study of the energy shift in relation to the particle size using

controlled dissolution has also not been reported, as well as a saturation in the maximum/minimum energy.

In this work, cyanide (inorganic ion) and cysteamine (alkane) are chosen, because they are strong nucleophiles, meaning that they have a strong ability to donate negative charge density to the silver. They both form a coordinative bond by donation of an electron pair, which generates a screening layer around the NPs. The free electrons of the NPs thereby shift towards the center, which increases the average electron density [1]. This results in a blueshift of the plasmon band, which is in accordance with a simple Drude model of the dielectric function.

Here, a correction factor, g , that accounts for a change in the conductivity is included in the expression of the dielectric constant [5]:

$$\varepsilon(\omega) = \varepsilon^\infty - \frac{g^2 \omega_p^2}{\omega^2 - i\omega\tau} \quad (1)$$

where ω_p is the bulk plasma frequency and τ is the free electron relaxation time. Dissolution in the presence of electron acceptors are also performed, by the use of hydrogen peroxide that is a stronger oxidizing agent than dissolved molecular oxygen.

2 RESULTS AND DISCUSSION

2.1 Materials and methods

Cyanide, cysteamine, hydrogen peroxide and sodium hydroxide was purchased from Sigma-Aldrich (Denmark) and used as received. Microscope slides (Menzel-Gläser, Thermo scientific, Germany) were sonicated in DI water for 10 min and piranha cleaned for 10 min ($\text{H}_2\text{SO}_4 / \text{H}_2\text{O}_2$ 3:1) prior to metal evaporation. Silver was evaporated at a pressure of 2×10^{-6} mBar with a calibrated evaporation rate of 2 \AA/s at thicknesses ranging from 0.5 nm to 10 nm. The samples were annealed under reducing conditions (30 sccm H_2 and 100 sccm N_2) at $400 \text{ }^\circ\text{C}$ in a vacuum furnace for 10 min. They were finally CO_2 -laser diced into 9 mm wide samples in order to fit into a 10 mm x 10 mm cuvette of the spectrophotometer (Shimadzu UV-1800, Japan).

TEM (Tecnai T20 G2, FEI), SEM (Supra40, Zeiss) and AFM (Nanoman, Bruker) was used for characterizing the films in terms of size and distribution. For the TEM imaging, grids with a 11 nm SiO_2 membrane were used.

The spectra were first recorded with DI water in the cuvette for 10-15 min to stabilize the signal and to obtain a reference spectrum of the sample. After addition of the samples, the spectra were recorded at 60 s intervals with a wavelength resolution of $\lambda=0.1 \text{ nm}$ in the range $\lambda=300\text{-}600 \text{ nm}$. Each spectrum took around 50 s to complete and 60-100 spectra were taken without drying or exchanging the

liquid in the cuvette of the spectrometer. No stirring or thermostating was used during the measurements.

2.2 Film characterization

The in-plane radius ranged from 3 nm (1 nm nominal thickness) to 60 nm (10 nm nominal thickness), while the height were around 3x the nominal deposited film thickness. This corresponds to the particles occupying around 1/3 of the surface area after annealing. Hence, the AgNPs had a smaller height than in-plane diameter. An example of a TEM micrograph is shown in figure 3 for the smallest deposited films thickness.

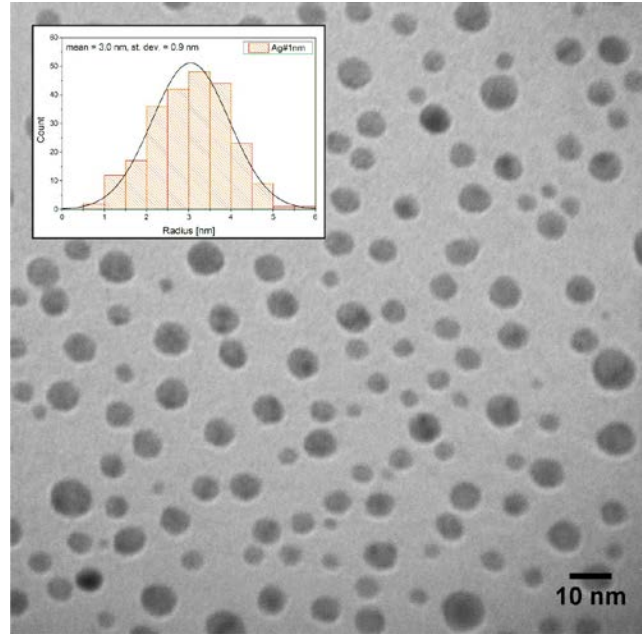


Figure 3. TEM micrograph of a 1 nm thick Ag film after vacuum annealing. The inserts shows a histogram with a normal fit of the particle size distribution.

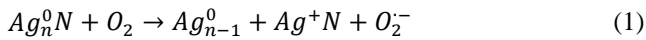
Table 1 shows the size distributions of some of the deposited AgNP film used during the experiments based on a normal fit. The name indicates the nominal deposited thickness.

Film name	Mean radius [nm]	Deviation [nm]
Ag#1nm	3.0	0.9
Ag#3nm	6.0	1.9
Ag#5nm	10.3	2.3
Ag#10nm	60	17

Table 1. Overview of particle sizes, investigated by TEM and SEM. The nominal deposited film thickness is given in their name.

2.3 Dissolution experiments

Two different types of dissolution schemes were applied in order to gradually decrease the NP size, while monitoring the plasmon band. In case of cyanide and cysteamine, so-called, nucleophile activated oxidative dissolution was employed. This is an indirect oxidation process, where binding of the ligand (electron pair donor), results in an increase in the free electron density of the bulk NP. This is equivalent to increasing the Fermi level [1] and decreasing the reduction potential. Basically, the free electrons are in a higher energy state, meaning that they can more easily be removed by the oxidizing agent. Hence, the oxidation rate (by dissolved O_2), dramatically increases. The reaction scheme is shown, here, which is similar to the well-known extraction of gold from metal ores by cyanide.



Ag_n^0 , denotes the zero-valent AgNPs consisting of n atoms, while N is the nucleophile bonded at the surface of the NPs. The superoxide radical, O_2^- , is formed as a result of the oxidation. In fig. 2 is shown an example of dissolution of a AgNP film immersed in a 100 μ M aqueous cyanide (pH=10).

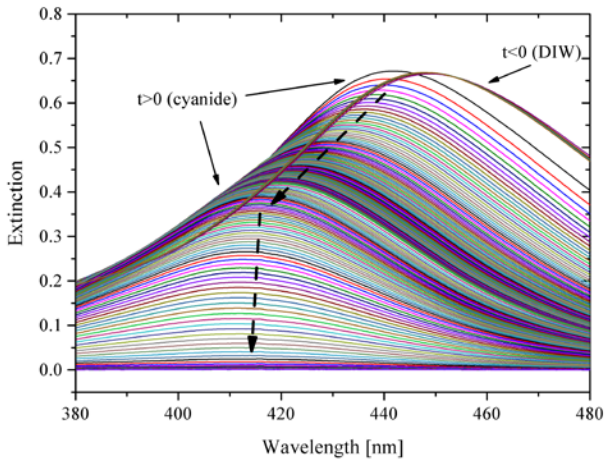


Figure 2. Extinction spectra during dissolution of an AgNP film (sample: Ag#5nm, table 1) using a 100 μ M aqueous cyanide solution. The dashed lines show the progression with time. The spectra without cyanide ($t < 0$, DI water) are also shown. The initial particle size was around 10 nm.

The negative electronic contribution from cyanide is very large, since no initial red shift is seen, even though the cyanide solution has a higher refractive index than DI water. A time trace of the peak position is shown in fig. 3, where an initial fast blue shift is seen.

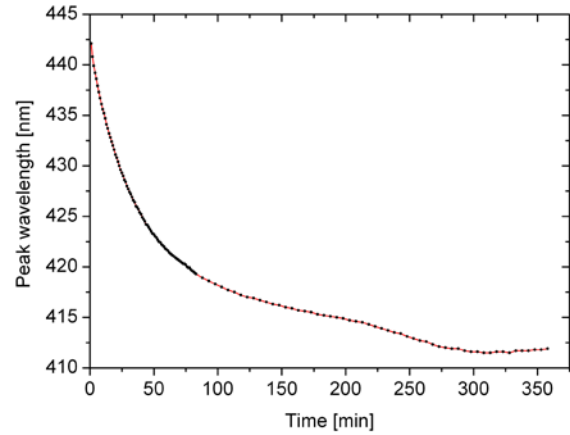


Figure 3. Time trace of the progression of the plasmon peak during dissolution of the AgNP film. Each black dot corresponds to one spectrum (Fig. 2).

Similar types of experiments were performed for both cysteamine and hydrogen peroxide, as described below.

2.4 Shifts in peak energy

Widely different theories (quantum size effects, nonlocal models etc [3, 4]) all typically predicts a $1/R$ -dependence of the peak energy, which is ascribed to the fundamental relation between the surface and the volume of the NPs [2]. Since the peak extinction of small spherical particles ($R < 5-10$ nm) scales with R^3 [1], the peak energy is furthermore plotted as a function of the inverse cube root of the peak extinction (fig. 4) in order to test for linearity.

An initial clear linear dependence is seen, which however quickly saturates at a maximum value around a total blueshift 0.22 eV (corresponds to a 17% increase in the free electron density calculated from the Drude model, equ. 1). The response should be compared with the blue trace, which shows the plasmon band for different NP sizes in the absence of ligands. The blue shift is expected since cyanide is a very strong electron density donor. There is no initial red shift, which indicates that the AgNPs are in the intrinsic domain from the onset of the experiment (meaning that electronic contributions dominate). The saturation in the energy shift is believed to be due to the onset of redox reactions with the solvent.

To setup an experiment that shows a transition from a traditional extrinsic response (dominated by the refractive index in the NP vicinity) to an intrinsic response, the ligand cysteamine was used ($NH_2-CH_2-CH_2-SH$). It is a weaker nucleophile than cyanide and should result in a larger refractive index change, since it is an alkane with a higher molecular weight. The formation of a self-assembled monolayer is seen by the initial red shift (extrinsic response), while for smaller particle sizes ($R < 3$ nm) a blue shift (in relation to the blue trace) is seen and it finally ends at the same blue shift as for cyanide (fig. 4).

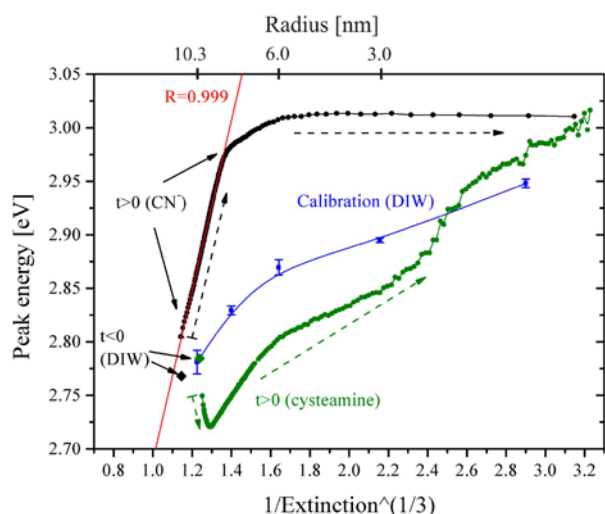


Figure 4. Peak extinction energy as a function of $1/\text{Ext}^{1/3}$, which is proportional to $1/R$, during controlled dissolution by binding with electron density donors in solution. A clear initial linear dependence as well as saturation at around 3.02 eV is seen for cyanide (100 μM , black trace). Cysteamine (1 mM, green trace) shows a initial red shift followed by a blue shift at the smallest NP sizes. Each dot corresponds to one spectrum (Fig. 2) and the dashed lines indicate the progression with time during decreasing the NP size. The calibration plot (blue trace) are for different sizes of NPs in DI water (no dissolution) and some of the radii are indicated on the top axis.

Experiments were furthermore performed to test for an increased red shift, by using hydrogen peroxide that is a stronger oxidizing agent than dissolved oxygen. The results in figure 5 are also interpreted as showing a transition from an extrinsic to an intrinsic response ($R < 6\text{nm}$). Initially, an increase in the refractive index of the solution, results in a constant red shift compared with blue calibration curve. However, at $R < 6\text{nm}$, the electronic contribution takes over and a large red shift is seen, indicating an electron spill-out effect, from discharging of the NPs. The red shift finally saturates, which also could be due to electrolysis of the water. Hence, a window of around $E=0.4$ eV can be utilized for monitoring of the plasmon band.

Typically gold is favored over silver, due to its higher stability in aqueous solution. However, by using controlled dissolution, more information can be obtained from the experiments. This can provide increased selectivity, without functionalization of the NPs. This is clearly seen by comparing cyanide and cysteamine (fig. 4). Both ligands start and end at the same positions, but the 'paths' taken are highly different. Hence, by utilizing the electronic contributions to the optical response, both the sensitivity and the selectivity can be increased, which of course is highly desirable for future plasmonic biosensor applications.

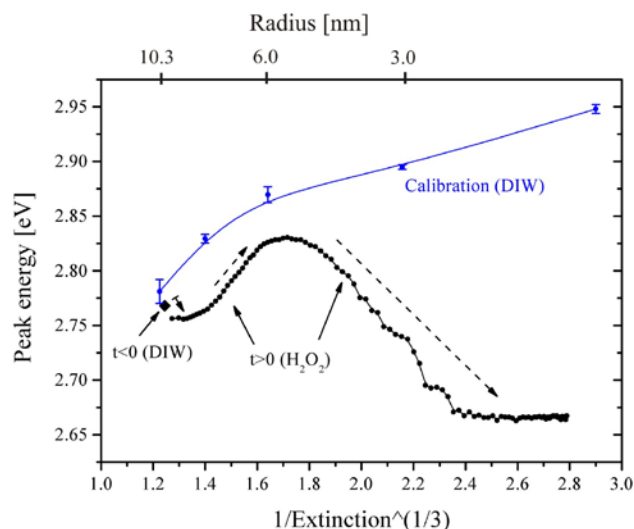


Figure 5. Peak extinction energy as a function of $1/\text{Ext}^{1/3}$, which is proportional to $1/R$, during controlled dissolution by binding with hydrogen peroxide (1 mM), which is an electron density acceptor / oxidizing agent. A clear transition from an extrinsic to an intrinsic domain is seen, by an initial constant red shift followed by a large red shift for the smallest NP sizes. Each dot corresponds to one spectrum (Fig. 2) and the dashed lines indicate the progression with time during decreasing the NP size. The calibration plot (blue trace) are for different sizes of NPs in DI water (no dissolution) and some of the radii from TEM are indicated on the top axis.

3 CONCLUSIONS AND OUTLOOK

Controlled oxidative dissolution has been utilized for investigation of both blue- and red shifts of the plasmon resonance of silver nanoparticles in aqueous solution. By also considering intrinsic electronic effects, additional information on the type of analyte can be obtained, compared to traditional refractive index sensing. In the future, models beyond the simple Drude description will be used to increase the knowledge of the system, while the chemistry will be further developed with the aim of improving the inherent selectivity and sensitivity of plasmonic sensing.

REFERENCES

- [1] A. Henglein, J. Phys. Chem., 97, p 5457, 1993.
- [2] U. Kreibig and M. Vollmer, 'Optical properties of metal clusters', Springer, 1995
- [3] S. Raza and N. A. Mortensen *et. al*, Nanophotonics, 2(2), p. 131, 2013.
- [4] R. C. Monreal, T. J. Antosiewicz and S. P. Apell, New Journal of Physics, 15, p. 083044, 2013.
- [5] Mandal *et al.*, J. Phys. Chem. C, 117 (13), p. 6741, 2013